Biomaterials 34 (2013) 5025–5035

Contents lists available at SciVerse ScienceDirect

Biomaterials

journal homepage: www.elsevier.com/locate/biomaterials

Osteogenic graft vascularization and bone resorption by VEGF-expressing human mesenchymal progenitors

Uta Helmrich [a], Nunzia Di Maggio [b], Sinan Güven [b], Elena Groppa [a], Ludovic Melly [a,c], Rene D. Largo [a,d], Michael Heberer [a,b], Ivan Martin [b], Arnaud Scherberich [b], Andrea Banfi [a,*]

[a] Cell and Gene Therapy, Department of Biomedicine and Department of Surgery, Basel University Hospital and Basel University, ICFS 407, Hebelstrasse 20, 4031 Basel, Switzerland
[b] Tissue Engineering, Department of Biomedicine and Department of Surgery, Basel University Hospital and Basel University, 4031 Basel, Switzerland
[c] Cardiac Surgery, Department of Surgery, Basel University Hospital, 4031 Basel, Switzerland
[d] Plastic and Reconstructive Surgery, Department of Surgery, Basel University Hospital, 4031 Basel, Switzerland

ARTICLE INFO

Article history:
Received 27 February 2013
Accepted 14 March 2013
Available online 6 April 2013

Keywords:
Angiogenesis
Bone tissue engineering
Mesenchymal stem cell
Osteoclast
Silicate-substituted apatite
VEGF

ABSTRACT

Rapid vascularisation of tissue-engineered osteogenic grafts is a major obstacle in the development of regenerative medicine approaches for bone repair. Vascular endothelial growth factor (VEGF) is the master regulator of vascular growth. We investigated a cell-based gene therapy approach to generate osteogenic grafts with an increased vascularization potential in an ectopic nude rat model *in vivo*, by genetically modifying human bone marrow-derived stromal/stem cells (BMSC) to express rat VEGF. BMSC were loaded onto silicate-substituted apatite granules, which are a clinically established osteoconductive material. Eight weeks after implantation, the vascular density of constructs seeded with VEGF-BMSC was 3-fold greater than with control cells, consisting of physiologically structured vascular networks with both conductance vessels and capillaries. However, VEGF specifically caused a global reduction in bone quantity, which consisted of thin trabeculae of immature matrix. VEGF did not impair BMSC engraftment *in vivo*, but strongly increased the recruitment of TRAP- and Cathepsin K-positive osteoclasts. These data suggest that VEGF over-expression is effective to improve the vascularization of osteogenic grafts, but also has the potential to disrupt bone homoeostasis towards excessive degradation, posing a challenge to its clinical application in bone tissue engineering.

1. Introduction

Tissue engineering is a promising strategy for the repair of large bone defects. For this purpose, bone marrow-derived mesenchymal stromal/stem cells (BMSC) constitute a rich source of osteoprogenitors [1]. However, one of the major limiting factors towards the clinical implementation of BMSC-based tissue-engineered osteogenic grafts is the need to rapidly provide a sufficient blood supply after implantation to ensure their engraftment. In fact, the lack of vascularization in the centre of large cell-loaded constructs invariably leads to ischaemia followed by necrosis [2,3]. Apart from managing the supply of nutrients and oxygen to the cells and the removal of metabolic products, necessary for the survival, growth and differentiation of the engrafted cells, blood vessels also allow the recruitment of highly-specialised cells, like circulating osteoprogenitors, haematopoietic stem cells or monocytes, which can contribute to tissue regeneration and remodelling [4–6].

Several approaches to accelerate vascularization of tissue-engineered bone grafts upon implantation are currently being investigated [7]. These include surgical techniques, like flap- or arteriovenous loop-fabrication [8–10], biomaterial-based methods, like nano-/micro-fibre combined scaffolds or scaffold microfabrication designed to facilitate vascular in-growth [10,11], as well as the co-culture of osteogenic and vasculogenic precursor cells inside the grafts [12–14]. Another strategy is the supply of pro-angiogenic factors [11]. Among these, Vascular Endothelial Growth Factor (VEGF) is the master regulator of vascular growth both in normal and pathological angiogenesis and is therefore the most attractive and well-characterized factor for inducing the therapeutic growth of new blood vessels [15]. On one hand, VEGF has a very short half-life *in vivo*, but on the other hand its expression needs to be sustained for approximately 4 weeks in order to allow the stabilization and persistence of newly formed vessels [16–18]. Therefore, the use of recombinant protein is challenging,

* Corresponding author. Fax: +41 61 265 3990.
E-mail address: Andrea.Banfi@usb.ch (A. Banfi).

0142-9612/$ – see front matter © 2013 Elsevier Ltd. All rights reserved.
http://dx.doi.org/10.1016/j.biomaterials.2013.03.040

since a continuous delivery of the factor is required. A stable, long-term production directly inside the tissue is more practically achieved by gene therapy, i.e. the delivery of the genetic sequence to allow a continuous secretion of the factor by the target cells [19].

Therefore, here we tested the hypothesis that sustained expression of VEGF by genetically modified human BMSC could generate osteogenic grafts with an increased pro-angiogenic potential and efficient bone formation *in vivo*.

2. Materials and methods

2.1. BMSC isolation and culture

Human primary BMSC were isolated from bone marrow aspirates. The aspirates were obtained from the iliac crest of healthy donors during routine orthopaedic surgical procedures according to established protocols, after informed consent by the patients and following protocol approval by the local ethical committee (EKBB, Ref. 78/07). Cells were isolated and cultured as described [20]. Briefly, after centrifugation, the pellet was washed in PBS (Invitrogen, Grand Island, NY, USA), resuspended in α-MEM medium (Invitrogen) containing 10% bovine serum (HyClone, South Logan, UT, USA) and 5 ng/ml FGF-2 (BD Biosciences, Basel, Switzerland) and plated at a density of 10^5 nucleated cells/cm^2. BMSC were cultured in 5% CO_2 at 37 °C. When 80–90% confluence was reached, cells were re-plated in a new dish at a density of 3000 cells/cm^2.

2.2. MSC genetic modification

Primary human BMSC were transduced according to a high-efficiency protocol we recently developed [21]. Briefly, starting on day 6 after plating, cells were transduced twice a day for a total of 4 rounds with bicistronic retroviral vectors carrying either the gene for rat $VEGF_{164}$ (rVEGF) linked to a truncated version of the rat CD8a by an internal ribosomal entry site, or truncated CD8a alone as a control [22]. For this purpose, BMSC were cultured in 60-mm dishes, incubated with retroviral vector supernatants supplemented with 8 μg/ml polybrene (Sigma–Aldrich, St. Louis, MO, USA) for 5 min at 37 °C. The dishes were then centrifuged at 1100 g for 30 min at room temperature and supernatants were replaced with fresh medium. All experiments were performed with freshly prepared viral supernatants.

2.3. Flow cytometry and cell-sorting

For phenotypic characterization of BMSC ($n = 3$ independent donors), cells were incubated for 20 min on ice, in PBS with 5% BSA. The antibodies used were: CD90-FITC, CD73-PE, CD31-FITC, CD34-APC, CD45-FITC, IgG1-FITC, IgG1-PE, IgG-APC (all from Becton, Dickinson and Company, Franklin Lakes, NJ), CD105-FITC (Serotec Ltd. Oxford, UK), VEGFR2-FITC (R&D Systems). All the antibodies were used at a dilution of 1:50, except CD105-FITC, which was used at 1:20. CD8a expression was assessed by staining with a FITC-conjugated anti-rat CD8a antibody (clone OX-8; BD Pharmingen, San José, CA, USA), using previously optimized staining conditions [22], i.e. 2 μg of antibody/10^6 cells in 200 μl of PBS with 5% BSA. Data were acquired with a FACSCalibur flow cytometer (BD Biosciences) and analysed by using FlowJo software (Tree Star, Ashland, OR, USA). Cell sorting was performed with an Influx cell sorter (BD Biosciences) after staining for CD8a according to the same protocol.

2.4. Enzyme-linked immunosorbent assay (ELISA)

VEGF production was quantified in cell culture supernatants using a Quantikine rat VEGF ELISA kit (R&D Systems Europe, Abingdon, UK). One millilitre of fresh medium was incubated on MSCs cultured in 60-mm dishes in duplicate ($n = 2$) for 4 h, filtered, and frozen. Results were normalized by the number of cells in each dish and the time of incubation.

2.5. In vivo implantation of osteogenic constructs

Osteogenic constructs were generated as previously described [23]. Briefly, 60 mm^3 of 1–2 mm silicate-substituted apatite granules (Actifuse®; Apatech-Baxter, Elstree, UK) where mixed with 5×10^5 BMSC embedded in a fibrin gel (Tisseel®; Baxter, Vienna, Austria), with a final concentration of 20 mg Fibrinogen/ml and 6 IU of Thrombin/ml. The resulting constructs were implanted subcutaneously in nude rats (RNu/Nu, Charles-River, Sulzfeld, Germany) as previously described [24]. Six constructs were implanted for each condition ($n = 6$), generated with cells from 3 independent donors (2 replicates/donor). After 8 weeks, animals were sacrificed by inhalation of CO_2 and constructs were explanted. Animals were treated in agreement with Swiss legislation and according to a protocol approved by the Veterinary Office of Canton Basel-Stadt (permission #2167).

2.6. Histological processing

Explanted constructs were washed with PBS and fixed for 4 h with freshly prepared 1% paraformaldehyde (Sigma–Aldrich) in PBS. Subsequently, the samples were decalcified according to an established protocol [25]. Briefly, granules were transferred into a PBS-based solution containing 7% w/v EDTA (Sigma–Aldrich) and 10% w/v sucrose (Sigma–Aldrich) and incubated at 37 °C on an orbital shaker. The solution was renewed daily for 5–21 days, until the samples were fully decalcified, as estimated by the degree of sample stiffness. Finally, the samples were embedded in OCT compound (Sakura Finetek, Torrance, CA, USA), frozen in freezing isopentane (Sigma) and 10 μm-thick sections were obtained with a cryotome.

2.7. Analysis of angiogenesis

To visualize blood vessels, immunofluorescence staining was performed with the following primary antibodies and dilutions: mouse-anti-rat CD31 (Clone TLD-3A12, 1:100; AbD Serotec, Düsseldorf, Germany), rabbit-anti-NG2 (1:200, Millipore, Zug, Switzerland) and mouse anti-Smooth Muscle Actin (Clone 1A4, 1:400; MPBiomedicals, Basel, Switzerland). Fluorophore-conjugated secondary antibodies (Invitrogen) were used at a concentration of 1:200.

The amount of blood vessels was quantified from CD31-stained sections. Three representative fluorescence images per sample ($n = 6$ samples/group) were acquired with an Olympus BX61 microscope (Olympus, Münster, Germany). Vessel length density (VLD) was measured with Cell·P software (Olympus) by tracing the total length of vessels in the fields and by normalizing it to the area of the fields.

2.8. Analysis of bone formation

Bone tissue was detected by staining sections with haematoxylin and eosin (H&E) and microscopic observation both under transmitted and fluorescent light as previously described [26,27]. In addition, the presence of mature bone matrix was examined with Masson trichrome staining (Réactifs RAL, Martillac, France), performed according to manufacturer's instructions. Sections were also immunostained using antibodies against Type I Collagen (1:10,000 dilution; Quartett Immunodiagnostika und Biotechnologie GmbH, Berlin, Germany) or Osteocalcin (1:200 dilution; Millipore, Temecula, CA, USA), followed by incubation with biotinylated goat anti-mouse and goat anti-rabbit secondary antibodies (both 1:200 dilution; Dako, Glostrup, Denmark) and ABC-alkaline phosphatase complex kit (Dako), Fast Red staining (Dako) and counterstaining with haematoxylin.

2.9. Assessment of cell engraftment

Human-specific Alu repeat DNA sequences were detected by *in situ* hybridization, according to a protocol adapted from a previously described procedure [28]. Briefly, a digoxigenin-labelled probe for the Alu sequence was prepared by PCR from 50 ng of human genomic DNA by incorporating a digoxigenin-labelled nucleotide (DIG-dUTP, Roche, Basel, Switzerland) in the reaction. The following primers were used: forward 5′-cgaggcgggtggatcatgaggt-3′, reverse 5′-ttttttgagacggagtctcgc-3′. After an initial denaturation step at 94 °C for 5 min, the reaction was carried out with 40 cycles consisting of a denaturation step at 95 °C for 15 s, an annealing step at 65 °C for 30 s and an elongation step at 72 °C for 30 s. The PCR product was purified using the QIAquick PCR Purification Kit (Quiagen, Hombrechtikon, Switzerland) according to the manufacturer's protocol. To perform *in situ* hybridization sections were first treated with 0.5 mg/ml Pepsin in 0.01 N HCl for 10 min at 37 °C and incubated in 0.1 M TEAC (Sigma–Aldrich) for 10 min at room temperature. Subsequently they were incubated for 30 min at 42 °C in pre-hybridization buffer containing 4× SSC, 50% deionized formamide, 1× Denhardt's solution, 5% dextrane sulphate and 0.2 μM bovine DNA. At the end of pre-hybridization, slides were incubated with fresh buffer containing 0.2 ng/μl digoxigenin-labelled probe. Following a denaturation step at 95 °C for 3 min and immediate cooling at 4 °C for 3 min, hybridization was carried out for 16 h at 42 °C in a wet chamber. Slides were then washed twice for 5 min in 2× SSC at room temperature and twice for 10 min at 42 °C in 0.1× SSC. Finally, the hybridized probe was detected by immunohistochemistry using anti-digoxigenin alkaline phosphatase-conjugated Fab fragments (Roche) and NBT/BCIP (Roche) as substrate. The sections were counterstained with nuclear fast red (Sigma).

The presence of endothelial structures of human origin, derived from the implanted human BMSC, was determined by staining with a biotin-conjugated specific anti-human CD34 antibody (QBEND/10; 1:50 dilution; Abcam Plc, Cambridge, UK). After incubation with ABC-alkaline phosphatase complex (Dako), specific staining was revealed by using Fast Red (Dako). Sections were counterstained with haematoxylin.

2.10. Osteoclast detection

In order to detect osteoclasts, sections were stained for tartrate-resistant acid phosphatase (TRAP) activity using the leucocyte acid phosphatase kit (Sigma–

Aldrich), according to manufacturer's instructions. Briefly, after rinsing with water, the slides were stained with 0.3 mg/ml Fast Red Violet LB dissolved in TRAP buffer (0.1 M sodium acetate, 0.1 M acetic acid, 1 mg/ml naphthol AS-MX phosphate, pH 5.0) for 1 h at 37 °C. After TRAP staining, nuclear counterstaining was performed with haematoxylin for 1 min at room temperature. TRAP-positive cells were quantified on 5 representative fields per construct in 2 constructs/condition ($n = 10$/condition). The percentage area occupied by TRAP-positive cells was determined using the ImageJ software (NIH, Bethesda, MD, USA) and normalized to the total area in each field.

In addition, the identity of detected osteoclasts was confirmed by Cathepsin K immunostaining on serial slides, as described [29]. Briefly, the staining was performed using a polyclonal anti-Cathepsin K antibody (1:1000, BioVision, Mountain View, CA, USA) over-night at 4 °C and a biotinylated goat anti-rabbit secondary antibody (1:200, Dako, Glostrup, Denmark) for 45 min at room temperature, followed by incubation with ABC-alkaline phosphatase complex (Vector Laboratories, Burlingame, CA, USA) and counterstaining with haematoxylin for 1 min at room temperature.

2.11. Statistics

Data were analysed with Prism 4.0a software (GraphPad, La Jolla, CA, USA) and results were presented as means ± standard error. The significance of differences was evaluated by analysis of variance (ANOVA) followed by the Bonferroni test. $P < 0.05$ was considered statistically significant.

3. Results

3.1. Generation of VEGF-expressing BMSC

Human BMSC were transduced to express rat VEGF linked to a truncated form of CD8a as a FACS-detectable cell surface marker (VEGF-BMSC). Rat VEGF was used in order to avoid an antibody response against the secreted factor after *in vivo* implantation in nude rats. Naïve BMSC and BMSC transduced with a retroviral vector expressing only the truncated CD8a marker (CD8-BMSC) were used as controls. Flow cytometry analysis showed that transduction efficiencies of >90% were routinely achieved by the first confluence, confirming our previous results [21]. At the first passage, the genetically modified BMSC were FACS-purified to eliminate non-transduced cells and to yield pure CD8-positive cell populations (data not shown).

At the moment of transduction (p0) naïve BMSC were homogeneously positive for expression of CD105, CD73 and CD90 (Table S1), which were previously described to identify mesenchymal progenitors in heterogeneous mesenchymal populations [30,31]. The presence of mature haematopoietic cells (CD45+) and endothelial cells (CD31+/CD34+ or VGFR2+) was extremely infrequent. In order to verify whether VEGF expression during *in vitro* culture before implantation could expand the few endothelial cells present, we analysed also p2 populations. We found that not only endothelial cells were not expanded, but essentially disappeared from all conditions (CD31+/CD34+: Naïve = 0.0 ± 0.0%, CD8 = 0.0 ± 0.0%, VEGF = 0.0 ± 0.0%; VEGFR2+: Naïve = 0.0 ± 0.0%, CD8 = 0.0 ± 0.0%, VEGF = 0.1 ± 0.1%).

3.2. Graft vascularization by extensively expanded VEGF-BMSC

For clinical applications, significant *in vitro* expansion of BMSC is required after isolation in order to obtain the large cell number necessary to generate osteogenic grafts of critical size. Therefore, we first investigated whether VEGF-expressing BMSC exhibited a stable potential to improve graft vascularization despite extensive expansion. *In vivo* bone formation and vascularization potential by genetically modified BMSC were investigated in an established model of osteogenic graft ectopic implantation in nude rats, in order to avoid confounding factors represented by ischaemia and an osteogenic environment. Implanted constructs were prepared by embedding silicate-substituted apatite granules within a fibrin gel containing cells, using commercially available materials widely accepted in the clinic for a variety of applications, including bone repair.

Production of VEGF protein by VEGF-BMSC was confirmed by ELISA (68.0 ± 18.7 ng/10^6cells/day of rat VEGF), whereas naïve and

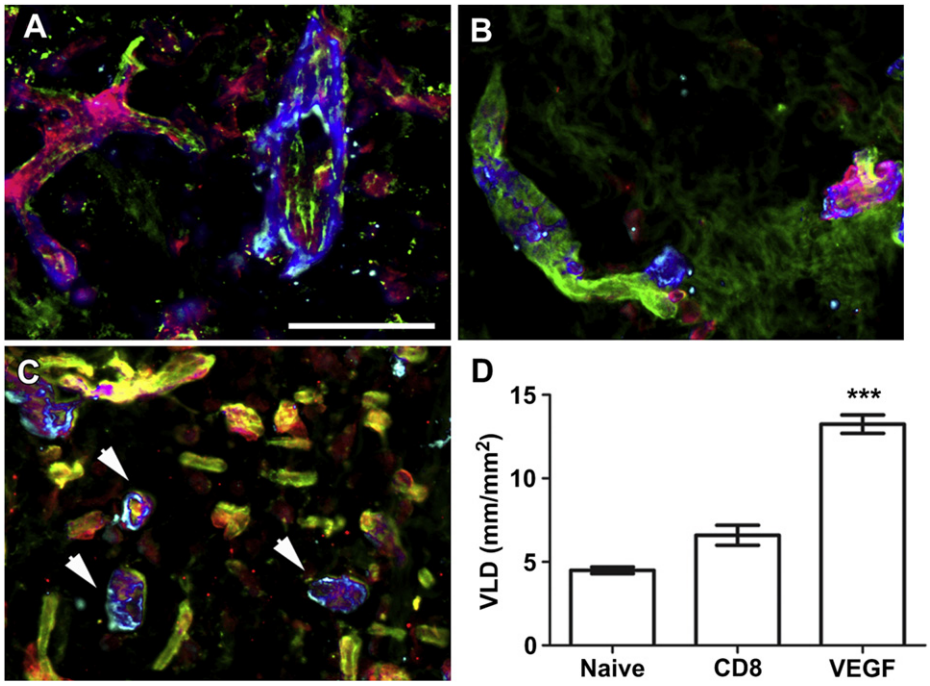

Fig. 1. *In vivo* angiogenesis by expanded VEGF-expressing BMSC. A–C, Immunofluorescence staining for endothelium (CD31, green), pericytes (NG2, red) and smooth muscle cells (SMA, blue) in sections of pellets made with fibrin and silicate-substituted apatite granules seeded with naïve BMSC (A), control CD8-BMSC (B) or VEGF-BMSC (C) 8 weeks after subcutaneous implantation in nude rats. Scale bar = 50 μm for all panels. White arrowheads indicate smooth muscle-covered arterioles. D, Quantification of the amount of induced angiogenesis. VLD = vessel length density, expressed as millimetres of vessel length per square millimetre of tissue area (mm/mm^2); ***=$p < 0.0001$ compared to both naïve and CD8 cells. (For interpretation of the references to colour in this figure legend, the reader is referred to the web version of this article.)

control CD8-BMSC did not secrete appreciable amounts (0.7 ± 0.3 and 0.5 ± 0.3 ng/10^6cells/day, respectively).

BMSC derived from 2 independent donors were thus cultured until p7 after transduction and FACS-purification, reaching a total of 30–35 population doublings. The cells were then seeded onto constructs made of silicate-substituted apatite granules and fibrin hydrogel, and implanted subcutaneously in nude rats for 8 weeks. An analysis of the vascularization inside the constructs by immunofluorescence staining showed that the control pellets loaded with either naïve or CD8-expressing BMSC contained mostly large-calibre regular vessels, covered with α-SMA-positive smooth muscle cells, similar to arterioles, and only a few capillaries with NG2-positive pericytes (Fig. 1A–B). Conversely, over-expression of VEGF resulted in extensive microvascular networks, associated with NG2-positive pericytes, and displaying the morphology of normal stable capillaries (Fig. 1C). Among these, a few arterioles of larger diameter covered by smooth muscle were also identified (white arrows in Fig. 1C), demonstrating the formation of a hierarchically structured vascular bed, with both conductance vessels for efficient flow and microvascular networks for metabolic exchange. Angiogenesis was quantified by measuring vessel length density, i.e. the total length of vessels in a given area independent of vessel diameter [16,32]. As shown in Fig. 1D, VEGF expression by BMSC induced a 2- to 3-fold increase in vessel length density, compared both to naïve and CD8-BMSC (13.2 ± 0.8 vs. 4.5 ± 0.3 and 6.6 ± 0.8 mm/mm^2, respectively; $p < 0.0001$ for both comparisons).

Analysis of bone tissue formation by H&E staining and fluorescent-light microscopy revealed only fibrous tissue, but no bone, in every constructs implanted with either control or VEGF-expressing BMSC (Fig. 2), consistently with the expected loss of BMSC differentiation potential after *in vitro* expansion for more than 30 population doublings [33].

3.3. Graft vascularization and bone formation by minimally expanded VEGF-BMSC

In order to determine the effects of VEGF over-expression on bone formation by transduced osteoprogenitors, BMSC expansion was minimized, so that their intrinsic osteogenic capacity would not be impaired by extensive *in vitro* culture. As shown in Fig. 3, two

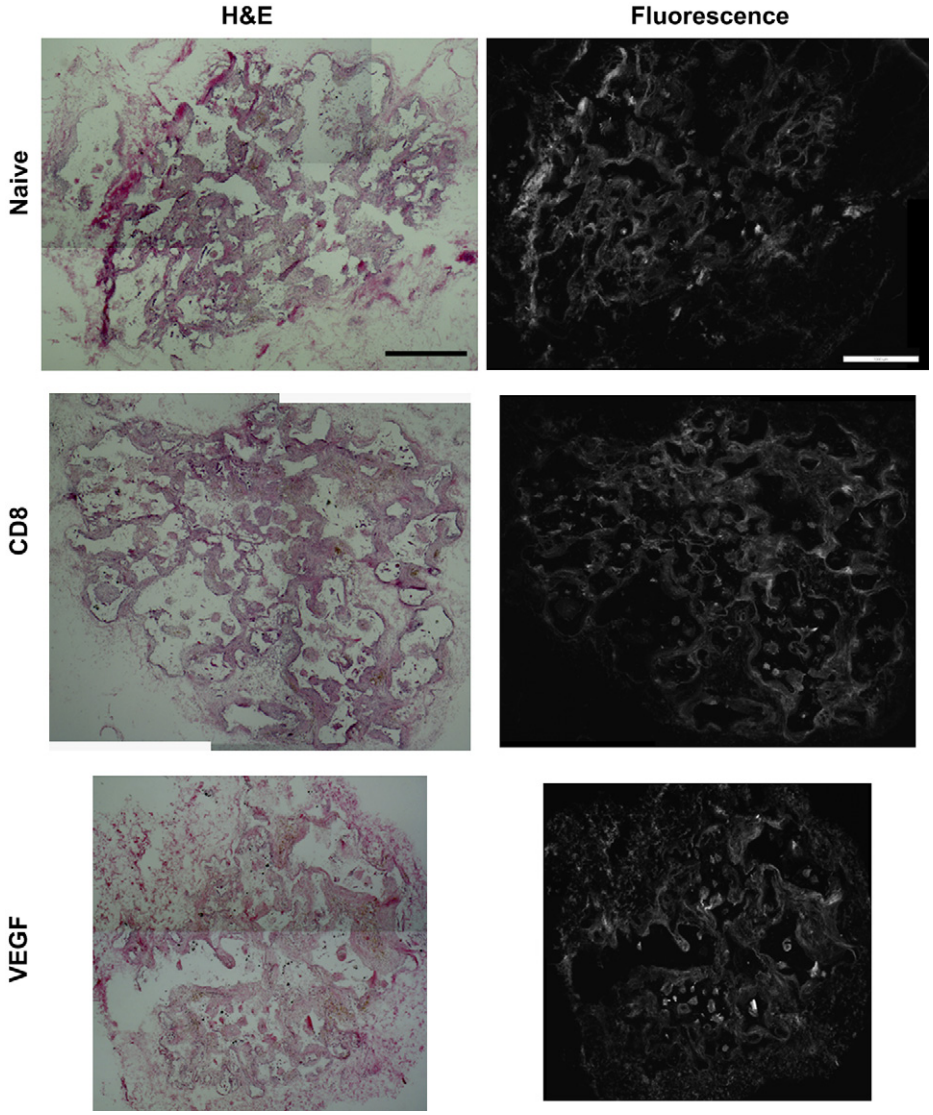

Fig. 2. *In vivo* bone formation by expanded VEGF-expressing BMSC. Composite images of entire sections of pellets seeded with naïve BMSC (Naive), CD8-BMSC (CD8) or VEGF-BMSC (VEGF), 8 weeks after subcutaneous implantation in nude rats. After staining with haematoxylin and eosin, sections were viewed under transmitted (H&E), as well as fluorescent light (Fluorescence). Scale bar = 1 mm in all panels.

conditions were investigated: 1) populations implanted at the earliest possible time, i.e. upon reaching the first confluence, which contained <10% non-transduced cells (p1, corresponding to 10.5 ± 0.5 population doublings); and 2) FACS-purification at the first passage to eliminate the few non-transduced cells, followed by implantation at the second passage (p2, corresponding to 13.5 ± 0.5 population doublings).

Grafts were explanted after 8 weeks to evaluate both blood vessel growth and bone tissue formation. Similarly to the results obtained with extensively expanded cells, control grafts generated with both p1 and p2 naïve or CD8-BMSC were vascularized by sparse vessels displaying characteristics of normal arterioles, with a regular smooth muscle coating, and only few pericyte-covered capillaries (Fig. 4A–D). Both p1 and p2 VEGF-expressing BMSC, on the other hand, significantly increased the amount of pericyte-covered microvascular networks, while preserving the presence of some arterioles (Fig. 4E–F). As shown in Fig. 4G, a quantification of vessel length density showed that VEGF-expressing BMSC induced a 2- to 3-fold increase in graft vascularization (p1 = 13.3 ± 1.1 and p2 = 13.1 ± 1.3 mm/mm^2; $p < 0.0001$ for all comparisons) compared to naïve (p1 = 5.7 ± 0.7 and p2 = 4.7 ± 0.6 mm/mm^2) and CD8-BMSC (p1 = 6.0 ± 0.5 and p2 = 4.5 ± 0.4 mm/mm^2). No difference in the amount of vascular growth induced was observed between p1 and p2 cells.

In order to investigate whether implanted human BMSC could contribute directly to the formation of endothelial structures, we took advantage of a monoclonal anti-CD34 antibody that recognizes specifically human endothelial cells, but not the rat counterparts (Fig. S1). Staining of human adipose tissue as positive control specifically identified CD34+ cells both in the endothelial and adventitial layers of blood vessels, as previously described [34]. However, no endothelial structure could be identified in any of the BMSC-loaded constructs that was fully or partially of human origin, suggesting that BMSC-derived endothelial cells do not account for the increased vascularization of VEGF-expressing osteogenic constructs.

Bone tissue was identified by analysis of H&E-stained sections with both transmitted light and fluorescence microscopy. In fact, the packed, parallel arrangement of collagen fibres present in bone lamellae specifically induces strong autofluorescence [27]. All constructs seeded with minimally expanded naïve or CD8-BMSC displayed abundant formation of bone tissue, both with p1 and p2 cells (Fig. 5A–D and G–J). This tissue was characterized by osteocyte lacunae, embedded in a very dense lamellar matrix, typical of the structure of mature bone (Fig. 5M–N). However, constructs seeded with VEGF-BMSC contained a severely reduced amount of bone compared to naïve or CD8-BMSC (Fig. 5E–F and K–L). In addition, the bone tissue formed by VEGF-BMSC was characterized by thin layers of osteoid with a less organized lamellar structure, suggesting a less mature matrix (Fig. 5O–P). Masson trichrome staining confirmed that the bone matrix in control conditions was mature, as evidenced by the high content in elastic fibres (red stain in Fig. 6A–D), whereas VEGF-BMSC constructs contained only immature bone tissue (green stain in Fig. 6E–F). Despite the differences in the relative amounts, the tissue generated by all conditions displayed positive expression of the bone matrix proteins Type I collagen and Osteocalcin (Fig. S2). Taken together, these results (Figs. 5, 6 and Fig. S2) unequivocally show that the induced tissue was not due to dystrophic calcification, but displays features of physiological bone tissue.

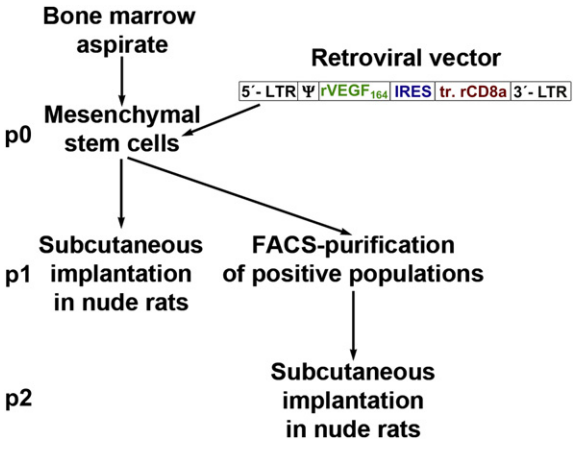

Fig. 3. Experimental design to investigate angiogenesis and bone formation by minimally expanded VEGF-expressing BMSC. BMSC were isolated and transduced (p0) with a bicistronic retroviral vector co-expressing rat $VEGF_{164}$ ($rVEGF_{164}$) and a truncated version of rat CD8a (tr.rCD8a). Implantation was performed either immediately after transduction, when cells reached the first confluence (p1), or after FACS-purification to eliminate the few non-transduced cells, one passage later (p2). LTR = retroviral Long Terminal Repeats; ψ = packaging signal; IRES = Internal Ribosomal Entry Sequence.

3.4. Stable engraftment of implanted BMSC

In order to determine whether the reduced bone formation observed with VEGF-expressing BMSC might be due to an impaired survival of the implanted osteoprogenitors, human BMSC were identified in histological sections by *in situ* hybridization with a probe for human-specific Alu repeat sequences in nuclear DNA. Constructs seeded with naïve and CD8-BMSC showed a homogeneous mixture of positive and negative cells within the bone tissue and the surrounding soft tissue, indicating the contribution of both the implanted BMSC and host-derived osteoprogenitors to bone formation (Fig. 7A–D). Human cells were similarly present in the constructs loaded with VEGF-expressing BMSC, both within the limited amount of bone tissue and in the surrounding soft tissue (Fig. 7E–F).

3.5. Osteoclast recruitment

The amount of bone tissue depends on the balance between deposition by osteoblasts and resorption by osteoclasts [35]. Therefore, in order to evaluate the bone-resorbing activity in the constructs, the amount of osteoclasts in the different conditions was quantified by staining for tartrate-resistant acid phosphatase (TRAP). In naïve and CD8-BMSC grafts, very few TRAP-positive cells were detected in contact or in close proximity to the bone matrix (Fig. 8A–D). However, constructs containing VEGF-expressing BMSC showed a highly increased density of TRAP-positive cells surrounding the thin bone lamellae (Fig. 8E–F). Quantification of the surface area occupied by TRAP-positive cells (Fig. 8G) showed that VEGF-expressing BMSC induced a 3- to 6-fold increase in osteoclasts (p1 = 2.0 ± 0.4% and p2 = 1.5 ± 0.2%; $p < 0.0001$ for all comparisons) compared to naïve (p1 = 0.4 ± 0.1% and p2 = 0.5 ± 0.1%) and CD8-BMSC (p1 = 0.3 ± 0.1% and p2 = 0.4 ± 0.1%). No significant difference was observed between p1 and p2 cells.

The identity of TRAP-positive cells was confirmed by immunostaining for Cathepsin K, a matrix-degrading protein specifically expressed by osteoclasts [29]. As shown in Fig. 9, Cathepsin K-positive cells were almost absent in constructs containing naïve BMSC, whereas they could be found in greatly increased numbers in constructs seeded with VEGF-BMSC, especially in close association with the newly formed ossicles or their remnants.

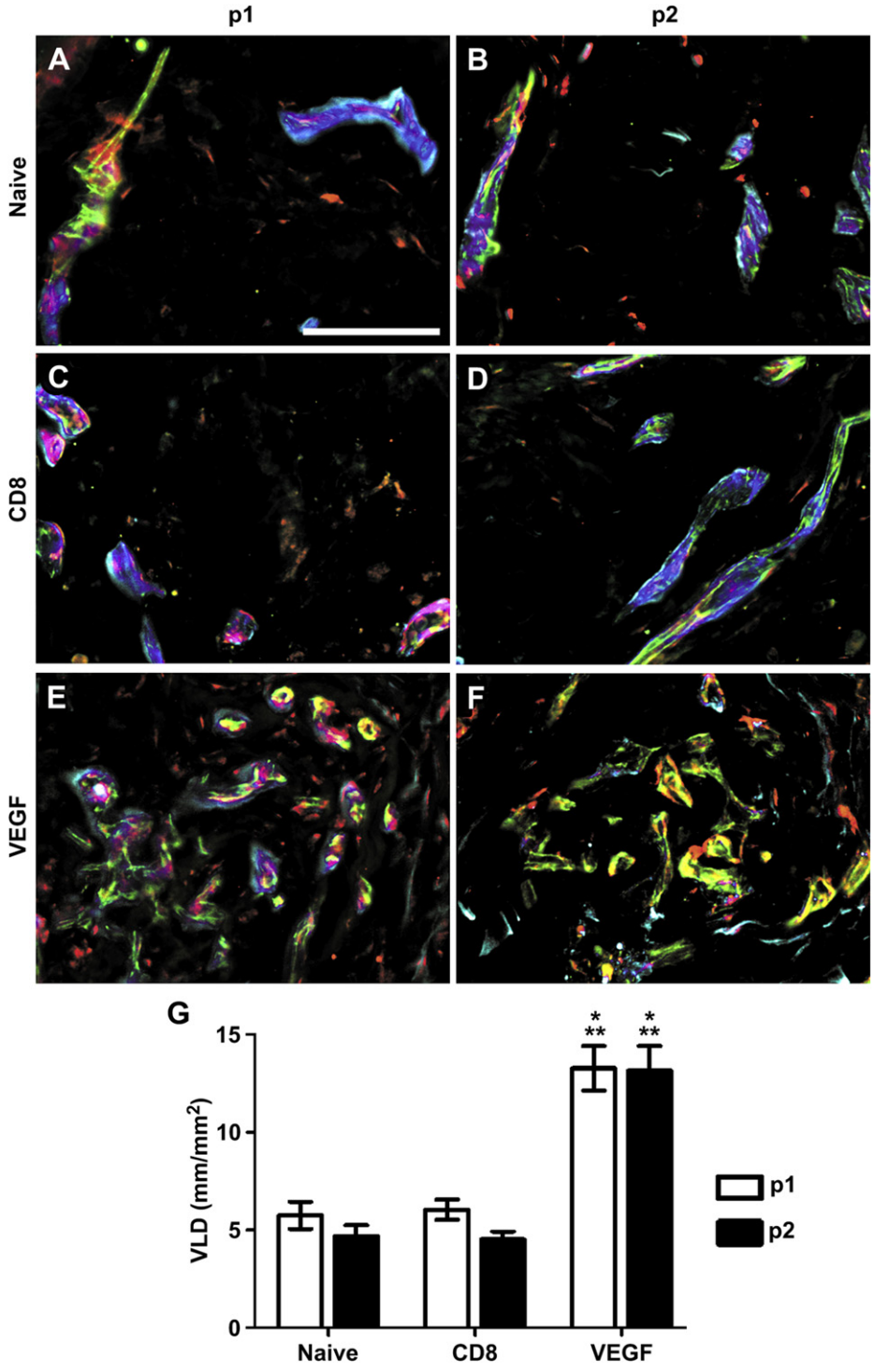

Fig. 4. *In vivo* angiogenesis by minimally expanded VEGF-expressing BMSC. A–F, Immunofluorescence staining for endothelium (CD31, green), pericytes (NG2, red) and smooth muscle cells (SMA, blue) in sections of pellets seeded with naïve BMSC (A–B), CD8-BMSC (C–D) or VEGF-BMSC (E–F), expanded for either 1 (p1) or 2 passages (p2), 8 weeks after subcutaneous implantation in nude rats. Scale bar = 50 μm in all panels. G, Quantification of the amount of induced angiogenesis. VLD = vessel length density, expressed as millimetres of vessel length per square millimetre of tissue area (mm/mm^2); ***=$p < 0.0001$. (For interpretation of the references to colour in this figure legend, the reader is referred to the web version of this article.)

4. Discussion

In this study we found that sustained over-expression of VEGF by genetically modified human BMSC was effective to improve vascularization of tissue-engineered bone grafts, leading to a 2- to 3-fold increase in vessel density compared to naïve cells and the generation of normal, mature and physiologically organized vascular networks. However, our data indicate that this approach also has the potential to substantially increase osteoclast recruitment and bone resorption, which led to a net decrease in the bone tissue mass.

Interestingly, VEGF over-expression caused not only an increase in the number of vessels, but also a qualitatively different

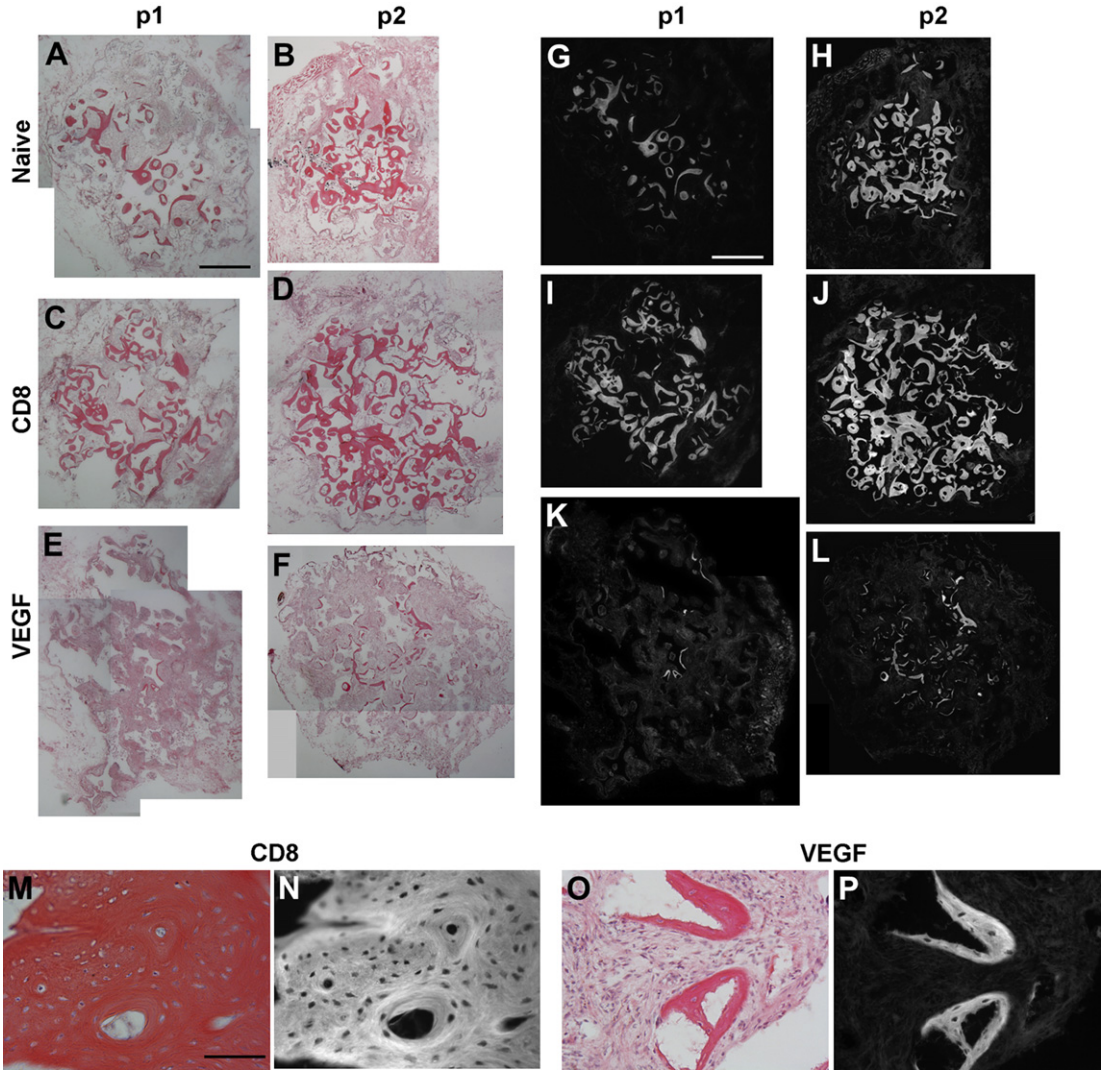

Fig. 5. *In vivo* bone formation by minimally expanded VEGF-expressing BMSC. A–L, Composite images of entire sections of pellets seeded with naïve BMSC (Naïve, A–B and G–H), CD8-BMSC (CD8, C–D and I–J) or VEGF-BMSC (VEGF, E–F and K–L), expanded for either 1 (p1) or 2 passages (p2), 8 weeks after subcutaneous implantation in nude rats. After staining with haematoxylin and eosin, sections were viewed under transmitted (A–F), as well as fluorescent light (G–L). Images of the same section are shown for each condition. Scale bar = 1 mm for all panels. M–P, High-magnification detail of the structure of bone matrix generated by control CD8-BMSC (M–N) or VEGF-BMSC (O–P) viewed under transmitted (M and O) and fluorescent (N and P) light. Images are taken from the sections shown in panels C, I, E and K, respectively. Scale bar = 100 μm for all panels.

composition of the vascular supply. In fact, grafts seeded with control cells contained mainly small arteries and veins, which efficiently carry blood flow (conductance vessels), but whose thick smooth muscle coating prevents metabolic exchanges with the tissue. VEGF-BMSC, on the other hand, generated physiologically structured vascular networks, composed of a few arterioles feeding into a large number of pericyte-covered capillaries, whose thin walls allow efficient exchange of respiratory gases and nutrients, as required to sustain a high metabolic demand by growing tissue.

Controversial results have been reported on the potential of BMSC to differentiate into endothelial cells either *in vitro* or *in vivo* [36]. Interestingly, blood vessels of human origin could not be found in any of the constructs. These results cannot exclude completely the possible presence of rare BMSC-derived endothelial cells in the implanted constructs, but certainly these appear to be extremely rare and unlikely to have functional relevance in these conditions. Furthermore, the absence of human-origin vasculature *in vivo* is consistent with the negligible frequency of endothelial-phenotype cells in the input BMSC populations.

The improvement in vascularization was not diminished by extensive *in vitro* expansion of the transduced BMSC up to 35 population doublings, showing that genetic modification conferred a stable angiogenic potential. As expected, these expanded BMSC lost their osteogenic potential [33,37]. However, their sustained capacity to induce vascularization could be useful in other applications, where effective expansion of the vascular bed is required, but not progenitor differentiation, such as in cell-based approaches for therapeutic angiogenesis in peripheral or coronary artery diseases [38].

By minimizing cell expansion, the osteogenic differentiation potential of BMSC was maintained, but a strong reduction in bone formation was observed when VEGF was over-expressed. CD8-BMSC, which underwent similar retroviral vector transduction and FACS-purification, generated bone tissue as efficiently as naïve BMSC, demonstrating the specificity of VEGF expression in this effect.

A reduced amount of bone can result either from decreased bone formation, through impairment either of BMSC engraftment or of

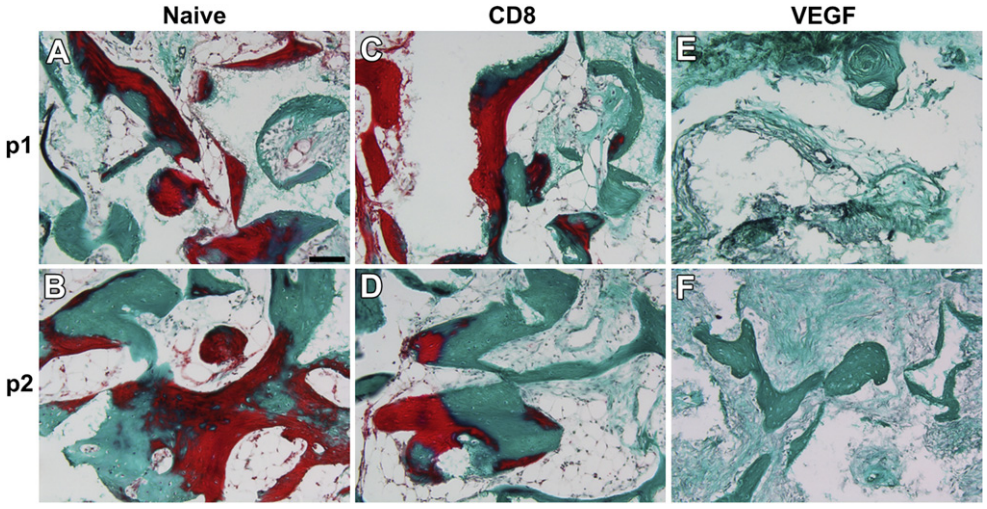

Fig. 6. Bone matrix maturation. Masson's trichrome staining of sections of pellets seeded with naïve BMSC (Naive, A–B), CD8-BMSC (CD8, C–D) or VEGF-BMSC (VEGF, E–F), expanded for either 1 (p1) or 2 passages (p2), 8 weeks after subcutaneous implantation in nude rats. Collagen fibres are stained green, while elastic fibres, characteristic of mature bone matrix, are stained red. Scale bar = 100 μm in all panels. (For interpretation of the references to colour in this figure legend, the reader is referred to the web version of this article.)

their osteogenic differentiation potential, or from increased resorption of the newly formed bone [35]. *In situ* hybridization for the human-specific Alu sequence demonstrated that VEGF-BMSC survived similarly to naïve cells and that they were found embedded in the bone matrix in an osteocyte position in all conditions. Furthermore, we also recently showed that VEGF over-expression did not impair the osteoblastic differentiation capacity of retrovirally-transduced human BMSC, as evidenced by the upregulation of the osteogenic-specific transcription factor Runx2 and calcium deposition *in vitro* [21]. On the other hand, here we found that VEGF over-expression specifically caused a greatly increased density of osteoclasts at the surface of bone areas, as identified by their specific positivity for Cathepsin K, which is not expressed by other myeloid cells involved in inflammatory responses [29]. Moreover, the ossicles found in VEGF-BMSC grafts were composed of thin trabeculae of immature matrix, suggesting that the tissue was constituted by newly deposited osteoid that did not yet remodel into mature bone. Taken together, these results suggest that VEGF over-expression caused a reduction in the amount and maturity of bone tissue rather through increased bone resorption than by impaired cell engraftment or differentiation of BMSC.

Bone formation and bone homoeostasis are highly connected with angiogenesis. VEGF upregulation is crucially required in osteochondral bone formation [39,40]. In addition, it has been shown that sustained VEGF over-expression promotes an increase in bone mass through direct stimulation of osteoblasts [41]. Several studies found a positive effect of VEGF on bone regeneration [42–44], while others did not observe any alteration in the osteogenic capacity of rabbit BMSC over-expressing VEGF after transduction with adeno-associated viral vectors [45]. On the other hand, Schonmeyr et al. recently showed that VEGF can inhibit the expression of the osteogenic trigger BMP-2 by rat BMSC in an autocrine and paracrine manner *in vitro*, although in this study the VEGF-expressing MSC did not survive *in vivo* and, therefore, it is

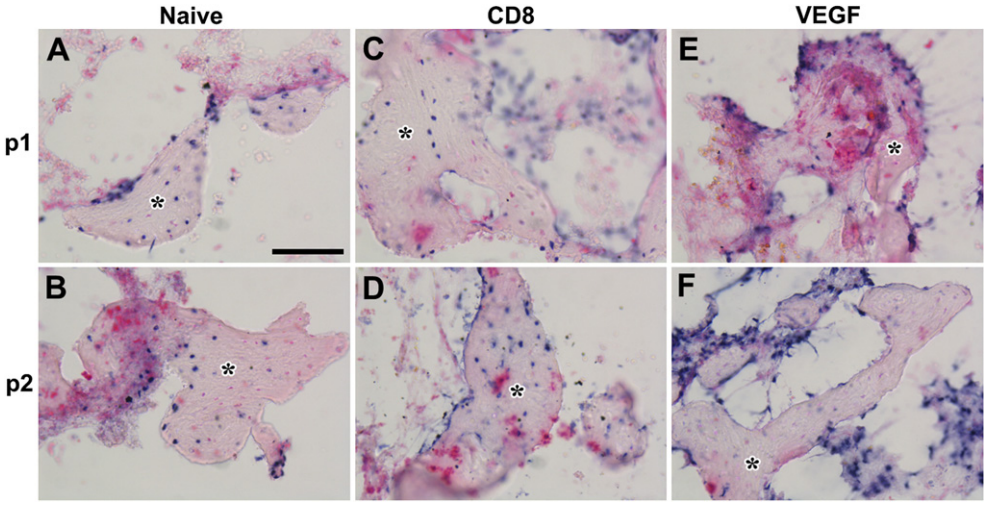

Fig. 7. *In vivo* survival of implanted BMSC. *In situ* hybridization for the human-specific Alu repeat sequences and counterstaining with nuclear fast red were performed on sections of pellets seeded with naïve BMSC (Naive, A–B), CD8-BMSC (CD8, C–D) or VEGF-BMSC (VEGF, E–F), expanded for either 1 (p1) or 2 passages (p2), 8 weeks after subcutaneous implantation in nude rats. Human nuclei are stained blue and mouse nuclei are stained red. Scale bar = 100 μm for all panels; asterisks (*) indicate bone tissue. (For interpretation of the references to colour in this figure legend, the reader is referred to the web version of this article.)

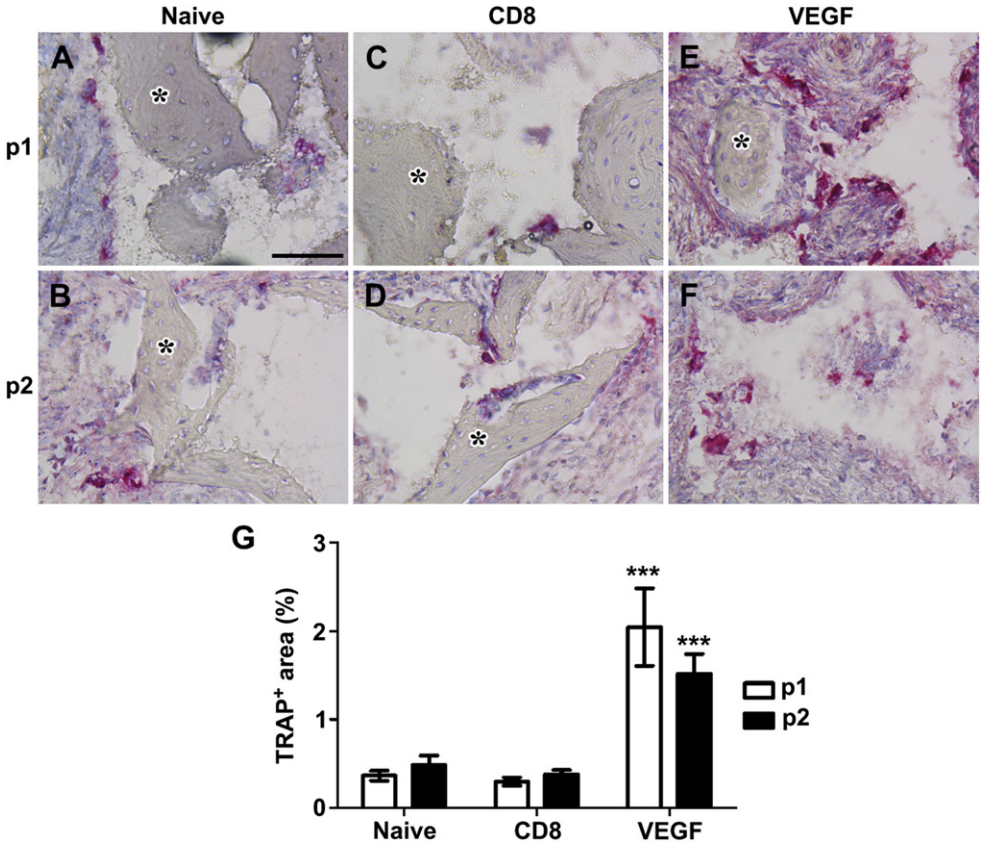

Fig. 8. Osteoclast activity detected by TRAP-staining. Histochemical stain for TRAP activity (red) and nuclear counterstaining with haematoxylin (blue) were performed on sections of pellets seeded with naïve BMSC (Naive, A–B), CD8-BMSC (CD8, C–D) or VEGF-BMSC (VEGF, E–F), expanded for either 1 (p1) or 2 passages (p2), 8 weeks after subcutaneous implantation in nude rats. Scale bar = 100 μm for all panels; asterisks (*) indicate bone tissue. G, Osteoclast recruitment was quantified by measuring the percentage area occupied by $TRAP^+$ cells normalized to the total area of each image (TRAP+ area (%)). ***=$p < 0.0001$. (For interpretation of the references to colour in this figure legend, the reader is referred to the web version of this article.)

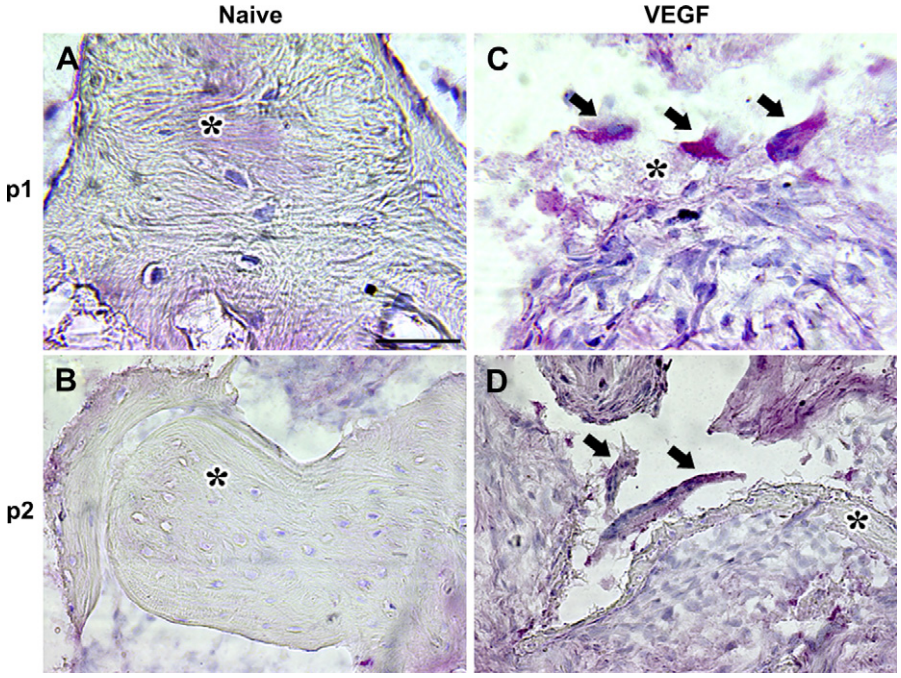

Fig. 9. Osteoclast activity detected by Cathepsin K-staining. Histochemical stain for Cathepsin K (red) and nuclear counterstaining with haematoxylin (blue) were performed on sections of pellets seeded with naïve BMSC (Naive, A–B) or VEGF-BMSC (VEGF, C–D), expanded for either 1 (p1) or 2 passages (p2), 8 weeks after subcutaneous implantation in nude rats. Scale bar = 100 μm for all panels; asterisks (*) indicate bone tissue; black arrows indicate Cathepsin-positive osteoclasts. (For interpretation of the references to colour in this figure legend, the reader is referred to the web version of this article.)

difficult to distinguish between failure of engraftment and inhibition of differentiation [46]. Furthermore, VEGF is a chemoattractant for the monocyte progenitors of osteoclasts in developing bone and has been shown to both support *in vitro* osteoclast differentiation and increase osteoclast survival and bone resorption [47,48]. In light of the sometime contradictory results reported in literature, the relationship between VEGF expression, vascularization, bone formation and bone resorption is certainly complex and likely to be context-dependent. It should be highlighted that our results were obtained in an established ectopic model with an osteo-conductive material widely used in the clinics, which allows the study of the intrinsic bone-forming capacity of the implanted cells without the influence of an osteogenic environment. Therefore, the data reported here show that VEGF over-expression has the potential to impair bone formation by unbalancing bone homoeostasis towards excessive resorption, which is clearly undesirable in a clinical setting. At least three parameters could be considered in order to devise strategies to uncouple these two functions and to preserve the positive effect on vascularization while avoiding the negative effect on bone formation: 1) the duration of VEGF expression; 2) its dose; and 3) the presence of an osteogenic environment.

VEGF expression is required only for about 4 weeks in order to generate persistent vessels [16,17] and it is possible that continued expression beyond this time, as caused by the constitutive retroviral promoter that was used here, is not necessary for vascularization, but only provides a continued stimulation of osteoclast recruitment. The use of inducible promoters, which can be switched off by systemic treatment with a drug [18], could address this point.

Further, the transduced BMSC that were employed here expressed heterogeneous levels of VEGF, as a result of the random integration of retroviral vectors in genomic areas with different transcriptional activities [21]. As normal angiogenesis can be induced over a wide range of VEGF levels up to a defined threshold dose [16], controlled expression at moderate levels might induce effective vascularization while limiting osteoclast recruitment. This could be achieved by using BMSC populations FACS-purified to homogeneously express specific VEGF levels, as we recently showed [21].

Subcutaneous implantation in an ectopic environment is a well-controlled experimental model. However, in physiological bone homoeostasis mechanical load provides crucial stimulation of anabolic osteoblastic activity and, in fact, lack of muscle activity causes severe bone rarefaction and osteoporosis [49]. Therefore, it will be interesting to test whether implantation in an orthotopic model, where the graft is subjected to the same mechanical load as the natural bone, the balance between bone formation and resorption might be restored.

5. Conclusions

Our data indicate that VEGF over-expression from genetically modified human BMSC is an effective strategy to improve the vascularization of osteogenic grafts, but also has the potential to impair bone tissue formation by increasing osteoclast recruitment and bone resorption. Therefore, the equilibrium between VEGF-triggered angiogenesis, osteogenesis and bone resorption needs to be carefully investigated in controlled models in order to devise rational strategies that exploit the pro-angiogenic potency of VEGF expression for a clinical application.

Acknowledgements

The authors gratefully acknowledge Francine Wolf (Basel University Hospital) for technical help with *in situ* hybridization and Dr. Andreas Goessl for generously supplying Tisseel® fibrin glue. This work was supported by an Intramural Research Grant of the Department of Surgery (Basel University Hospital), by the European Union FP7 grant MAGISTER (CP-IP 214685) and by the Swiss National Science Foundation grants 127426 and 143898 to A.B. and grants 120432 and 138519 to A.S. and I.M.

Appendix A. Supplementary material

Supplementary data related to this article can be found online at http://dx.doi.org/10.1016/j.biomaterials.2013.03.040.

References

[1] Marolt D, Knezevic M, Novakovic GV. Bone tissue engineering with human stem cells. Stem Cell Res Ther 2010;1:10.
[2] Kneser U, Stangenberg L, Ohnolz J, Buettner O, Stern-Straeter J, Mobest A, et al. Evaluation of processed bovine cancellous bone matrix seeded with syngenic osteoblasts in a critical size calvarial defect rat model. J Cell Mol Med 2006;10:695–707.
[3] Scheufler O, Schaefer DJ, Jaquiery C, Braccini A, Wendt DJ, Gasser JA, et al. Spatial and temporal patterns of bone formation in ectopically pre-fabricated, autologous cell-based engineered bone flaps in rabbits. J Cell Mol Med 2008;12:1238–49.
[4] Gerber HP, Ferrara N. Angiogenesis and bone growth. Trends Cardiovasc Med 2000;10:223–8.
[5] Brandi ML, Collin-Osdoby P. Vascular biology and the skeleton. J Bone Miner Res 2006;21:183–92.
[6] Eghbali-Fatourechi GZ, Lamsam J, Fraser D, Nagel D, Riggs BL, Khosla S. Circulating osteoblast-lineage cells in humans. N Engl J Med 2005;352:1959–66.
[7] Kanczler JM, Oreffo RO. Osteogenesis and angiogenesis: the potential for engineering bone. Eur Cell Mater 2008;15:100–14.
[8] Kneser U, Schaefer DJ, Polykandriotis E, Horch RE. Tissue engineering of bone: the reconstructive surgeon's point of view. J Cell Mol Med 2006;10:7–19.
[9] Scherberich A, Muller AM, Schafer DJ, Banfi A, Martin I. Adipose tissue-derived progenitors for engineering osteogenic and vasculogenic grafts. J Cell Physiol 2010;225:348–53.
[10] Santos MI, Reis RL. Vascularization in bone tissue engineering: physiology, current strategies, major hurdles and future challenges. Macromol Biosci 2010;10:12–27.
[11] Kanczler JM, Ginty PJ, White L, Clarke NMP, Howdle SM, Shakesheff KM, et al. The effect of the delivery of vascular endothelial growth factor and bone morphogenic protein-2 to osteoprogenitor cell populations on bone formation. Biomaterials 2010;31:1242–50.
[12] Koob S, Torio-Padron N, Stark GB, Hannig C, Stankovic Z, Finkenzeller G. Bone formation and neovascularization mediated by mesenchymal stem cells and endothelial cells in critical-sized calvarial defects. Tissue Eng Part A 2011;17:311–21.
[13] Buschmann J, Welti M, Hemmi S, Neuenschwander P, Baltes C, Giovanoli P, et al. Three-dimensional co-cultures of osteoblasts and endothelial cells in DegraPol foam: histological and high-field magnetic resonance imaging analyses of pre-engineered capillary networks in bone grafts. Tissue Eng Part A 2011;17:291–9.
[14] Gueven S, Mehrkens A, Saxer F, Schaefer DJ, Martinetti R, Martin I, et al. Engineering of large osteogenic grafts with rapid engraftment capacity using mesenchymal and endothelial progenitors from human adipose tissue. Biomaterials 2011;32:5801–9.
[15] Yla-Herttuala S, Rissanen TT, Vajanto I, Hartikainen J. Vascular endothelial growth factors – biology and current status of clinical applications in cardiovascular medicine. J Am Coll Cardiol 2007;49:1015–26.
[16] Ozawa CR, Banfi A, Glazer NL, Thurston G, Springer ML, Kraft PE, et al. Microenvironmental VEGF concentration, not total dose, determines a threshold between normal and aberrant angiogenesis. J Clin Invest 2004;113:516–27.
[17] Dor Y, Djonov V, Abramovitch R, Itin A, Fishman GI, Carmeliet P, et al. Conditional switching of VEGF provides new insights into adult neovascularization and pro-angiogenic therapy. Embo J 2002;21:1939–47.
[18] Tafuro S, Ayuso E, Zacchigna S, Zentilin L, Moimas S, Dore F, et al. Inducible adeno-associated virus vectors promote functional angiogenesis in adult organisms via regulated vascular endothelial growth factor expression. Cardiovasc Res 2009;83:663–71.
[19] Rissanen TT, Yla-Herttuala S. Current status of cardiovascular gene therapy. Mol Ther 2007;15:1233–47.
[20] Galotto M, Berisso G, Delfino L, Podesta M, Ottaggio L, Dallorso S, et al. Stromal damage as consequence of high-dose chemo/radiotherapy in bone marrow transplant recipients. Exp Hematol 1999;27:1460–6.
[21] Helmrich U, Marsano A, Melly L, Wolff T, Christ L, Heberer M, et al. Generation of human adult mesenchymal stromal/stem cells expressing defined

xenogenic vascular endothelial growth factor levels by optimized transduction and flow cytometry purification. Tissue Eng Part C Methods 2012;18:283–92.
[22] Wolff T, Mujagic E, Gianni-Barrera R, Fueglistaler P, Helmrich U, Misteli H, et al. FACS-purified myoblasts producing controlled VEGF levels induce safe and stable angiogenesis in chronic hind limb ischemia. J Cell Mol Med 2012;16:107–17.
[23] Mehrkens A, Saxer F, Mueller AM, Gueven S, Schaefer DJ, Heberer M, et al. Successful one-step engineering of osteogenic grafts with cells freshly isolated from human adipose tissue. Br J Surg 2010;97:S38.
[24] Scherberich A, Galli R, Jaquiery C, Farhadi J, Martin I. Three-dimensional perfusion culture of human adipose tissue-derived endothelial and osteoblastic progenitors generates osteogenic constructs with intrinsic vascularization capacity. Stem Cells 2007;25:1823–9.
[25] Kusser KL, Randall TD. Simultaneous detection of EGFP and cell surface markers by fluorescence microscopy in lymphoid tissues. J Histochem Cytochem 2003;51:5–14.
[26] Mueller AM, Davenport M, Verrier S, Droeser R, Alini M, Bocelli-Tyndall C, et al. Platelet lysate as a serum substitute for 2D static and 3D perfusion culture of stromal vascular fraction cells from human adipose tissue. Tissue Eng Part A 2009;15:869–75.
[27] Martin I, Mastrogiacomo M, De Leo G, Muraglia A, Beltrame F, Cancedda R, et al. Fluorescence microscopy imaging of bone for automated histomorphometry. Tissue Eng 2002;8:847–52.
[28] Kasten P, Vogel J, Luginbuhl R, Niemeyer P, Tonak M, Lorenz H, et al. Ectopic bone formation associated with mesenchymal stem cells in a resorbable calcium deficient hydroxyapatite carrier. Biomaterials 2005;26:5879–89.
[29] Chai YC, Roberts SJ, Desmet E, Kerckhofs G, van Gastel N, Geris L, et al. Mechanisms of ectopic bone formation by human osteoprogenitor cells on CaP biomaterial carriers. Biomaterials 2012;33:3127–42.
[30] Boiret N, Rapatel C, Veyrat-Masson R, Guillouard L, Guerin JJ, Pigeon P, et al. Characterization of nonexpanded mesenchymal progenitor cells from normal adult human bone marrow. Exp Hematol 2005;33:219–25.
[31] Sacchetti B, Funari A, Michienzi S, Di Cesare S, Piersanti S, Saggio I, et al. Self-renewing osteoprogenitors in bone marrow sinusoids can organize a hematopoietic microenvironment. Cell 2007;131:324–36.
[32] Thurston G, Suri C, Smith K, McClain J, Sato TN, Yancopoulos GD, et al. Leakage-resistant blood vessels in mice transgenically overexpressing angiopoietin-1. Science 1999;286:2511–4.
[33] Banfi A, Muraglia A, Dozin B, Mastrogiacomo M, Cancedda R, Quarto R. Proliferation kinetics and differentiation potential of ex vivo expanded human bone marrow stromal cells: implications for their use in cell therapy. Exp Hematol 2000;28:707–15.
[34] Crisan M, Corselli M, Chen WC, Peault B. Perivascular cells for regenerative medicine. J Cell Mol Med 2012;16:2851–60.
[35] Feng X, McDonald JM. Disorders of bone remodeling. Annu Rev Pathol 2011;6:121–45.
[36] Bianco P, Robey PG, Saggio I, Riminucci M. "Mesenchymal" stem cells in human bone marrow (skeletal stem cells): a critical discussion of their nature, identity, and significance in incurable skeletal disease. Hum Gene Ther 2010;21:1057–66.
[37] DiGirolamo CM, Stokes D, Colter D, Phinney DG, Class R, Prockop DJ. Propagation and senescence of human marrow stromal cells in culture: a simple colony-forming assay identifies samples with the greatest potential to propagate and differentiate. Br J Haematol 1999;107:275–81.
[38] Hodgkinson CP, Gomez JA, Mirotsou M, Dzau VJ. Genetic engineering of mesenchymal stem cells and its application in human disease therapy. Hum Gene Ther 2010;21:1513–26.
[39] Gerber HP, Hillan KJ, Ryan AM, Kowalski J, Keller GA, Rangell L, et al. VEGF is required for growth and survival in neonatal mice. Development 1999;126:1149–59.
[40] Zelzer E, Olsen BR. The genetic basis for skeletal diseases. Nature 2003;423:343–8.
[41] Maes C, Goossens S, Bartunkova S, Drogat B, Coenegrachts L, Stockmans I, et al. Increased skeletal VEGF enhances beta-catenin activity and results in excessively ossified bones. Embo J 2010;29:424–41.
[42] Street J, Bao M, deGuzman L, Bunting S, Peale FV, Ferrara N, et al. Vascular endothelial growth factor stimulates bone repair by promoting angiogenesis and bone turnover. Proc Natl Acad Sci U S A 2002;99:9656–61.
[43] Hiltunen MO, Ruuskanen M, Huuskonen J, Mahonen AJ, Ahonen M, Rutanen J, et al. Adenovirus-mediated VEGF-A gene transfer induces bone formation in vivo. FASEB J 2003;17:1147–9.
[44] Casap N, Venezia NB, Wilensky A, Samuni Y. VEGF facilitates periosteal distraction-induced osteogenesis in rabbits: a micro-computerized tomography study. Tissue Eng Part A 2008;14:247–53.
[45] Zhang C, Wang KZ, Qiang H, Tang YL, Li QA, Li MA, et al. Angiopoiesis and bone regeneration via co-expression of the hVEGF and hBMP genes from an adeno-associated viral vector in vitro and in vivo. Acta Pharmacol Sin 2010;31:821–30.
[46] Schonmeyr BH, Soares M, Avraham T, Clavin NW, Gewalli F, Mehrara BJ. Vascular endothelial growth factor inhibits bone morphogenetic protein 2 expression in rat mesenchymal stem cells. Tissue Eng Part A 2010;16:653–62.
[47] Niida S, Kaku M, Amano H, Yoshida H, Kataoka H, Nishikawa S, et al. Vascular endothelial growth factor can substitute for macrophage colony-stimulating factor in the support of osteoclastic bone resorption. J Exp Med 1999;190:293–8.
[48] Yang QL, McHugh KP, Patntirapong S, Gu XS, Wunderlich L, Hauschka PV. VEGF enhancement of osteoclast survival and bone resorption involves VEGF receptor-2 signaling and beta(3)-integrin. Matrix Biol 2008;27:589–99.
[49] Lau R, Guo X. A review on current osteoporosis research: with special focus on disuse bone loss. J Osteopor 2011;2011:293808.